EXPERIMENTAL INVESTIGATION OF PULSATILE FLOW THROUGH AXISYMMETRIC CONSTRICTIONS

S.A. Abdallah, M.A. Shawky, H.A. Warda, and A.A. Hassan
Mechanical Engineering Department,
Faculty of Engineering, Alexandria University,
Alexandria, Egypt

Abstract

An experimental study has been conducted to acquire a better understanding of the characteristics of pulsatile flow through axisymmetric constrictions. The study was motivated by an interest in the fluid dynamics associated with constrictions frequently encountered in the cardiovascular system. Acoordingly the experimental work was carried out within a range of frequencies of oscillation covering those physiologically relevant, and a range of area ratios which covers a sizable portion of the physiological range. Simultaneous measurements of pressure drop across the constriction and the downstream center line velocity are recorded. Profiles of peak velocity and temporal variation of axial velocity across the pipe in the downstream region were also obtained.

INTRODUCTION

The problem of analyzing the flow through cardiovascular constrictions, arterial or valvular, has challenged many engineers and physicians due to the envolvement of many complicating factors such as unsteadiness, turbulence, wall elasticity and separation. Surprising as it may appear to fluid mechanicians , most of the hydrodynamic studies in this field have not yielded a comprehensive information on the flow field.

The earliest approach to the problem was made by Dow [1] who suggested that the resistance of a constricted pulmonary valve can be estimated by applying the Poisseuille equation relating the pressure drop and flow rate across the constricted area. Later, Gorlin and Gorlin [2] proposed that the hydraulic formula for steady flow through nozzles or orifices with an empirically derived constant is adequate to estimate the area of stenotic valves .

More comprehensive in-vitro experimental works were later conducted to study the effect of different parameters such as the Reynolds number, the geometry of obstruction, the percentage of area reduction or the presence of more than one constriction in series, on the separation and reattachment points and on the pressure drop across the constriction [3-6] .

The ability to describe the flow through a partial occlusion adds to the insight needed to solve the puzzle of the genesis of atherosclerosis . Hence numerical computational solutions for the problem were presented by many researchers in the field [7-11]. These studies provided a better understanding of the basic fluid-mechanics phenomena. However, the assumptions of a steady, low Reynolds number laminar flow or a flow through plane conduit, restrict the direct application of the results to the in-vivo situation .

Many investigators have focused their attention on studying the turbulent flow field of the emerging jet in an attempt to develop a simple clinical technique to assess the severity of constrictions by analyzing the noise or murmur generated by the turbulent pressure fluctuations [12-16].

The recent advent of Doppler-echocardiography allowed the measurement of blood velocity in the cardiac chambers and great blood vessels. A non-invasive technique was thus developed to assess the severity of stenoses by measuring the jet exit velocity and applying Bernoulli's equation for steady flow. Numerous studies to correlate the Doppler derived and the measured pressure drop by catheterization, has been published [17-21].

Validation of the Doppler derived pressure gradient in an in-vitro experiment was carried out by Requarth et al.[22] in a steady flow loop by comparing the pressure loss across orifices of different area ratios with the simplified form of Bernoulli's equation .

The purpose of the present work is to investigate the relationship between the pulsatile pressure drop through a constriction and the fluctuating velocity in the near downstream region of the jet exit. This was conducted in an in-vitro experiment under controlled flow conditions that allow for studying the effect of periodicity and area ratios on the flow characteristics .

Experimental Set-up

The experimental set-up used in this study is shown schematically in Figure(1). It consists of a constant level elevated tank feeding constant flow rate of water to the circuit through a control valve. Simple harmonic oscillations are superimposed on the flow using a piston-cylinder combination driven by a variable speed electric motor and reducing pulleys through a scotch-Yoke mechanism. This system was adopted to obtain pulsating frequencies of 0.5, 0.7, 1, 1.4 and 2 cps. The generated pulsatile flow passes in a 1" pipe to the test section.

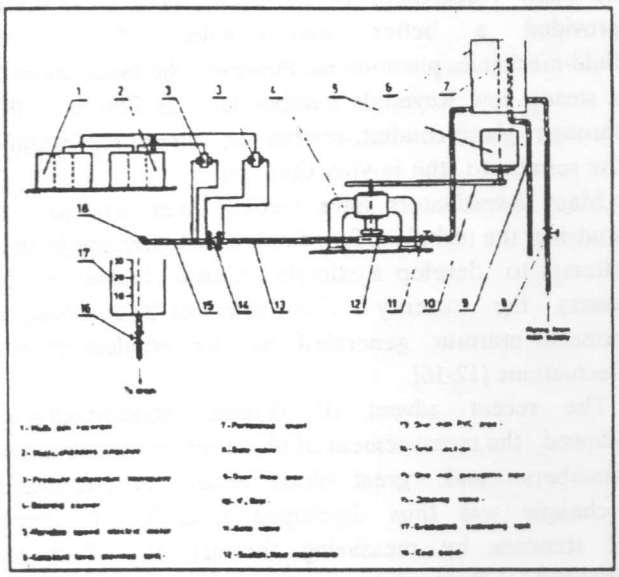

Figure 1. General layout of the experimental apparatus.

The test section consists of an interchangeable nozzle fixed between two nozzle holders. The nozzles have the same inlet diameter (D) of 1" and length (L) of 1", while the diameter at the outlet (d) varies in order to give outlet to inlet diameter ratios of 0.25, 0.4, 0.6 and 0.8 . The flow downstream of the test section is collected in a plexiglass graduated tank.

The pressure drop across the nozzle is measured using a differential pressure transducer. The core velocity at nozzle exit is measured simultaneously with the pressure drop across the tested nozzle using a calibrated pitot-static tube connected to another pressure transducer. Both transducers are identical, inductive type having a working range of 0-0.1 bar. The output signals of both transducers were amplified by a multi-channel amplifier, and then recorded using a multi-pen strip chart recorder.

The axial velocity was measured at different successive positions from r/R equal zero to r/R equal 0.9. Nea the wall the water velocity could not be measured due to the pitot-static tube thickness. The symmetry around the pipe axis was checked by measuring the velocity along the whole diameter to ensure the coincidence of the geometrical axis of the pipe with the axis of symmetry for the velocity distribution. To increase the accuracy, smaller distances between the points of measurements are chosen at regions of high velocity gradients.

RESULTS AND DISCUSSION

Samples of the recorded signals representing the pressure drop across the constriction and the simultaneously measured core-velocity downstream of the nozzle exit are shown in Figure (2). From similar figures corresponding to each tested nozzle at a certain frequency, pressure drop ΔP_n, and core velocity U_{cl} and peak to trough amplitudes of pressure drop ΔP_n and velocity U_{cl} could be obtained , as shown in Figure (3).

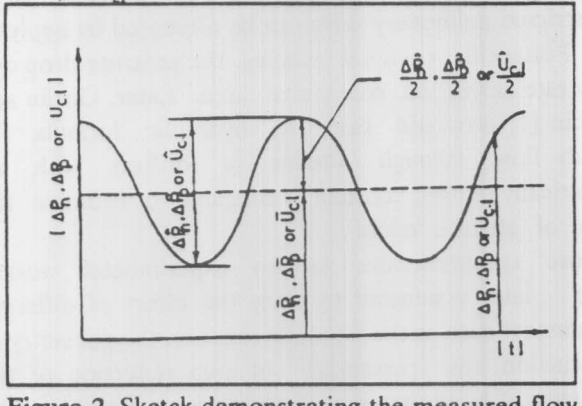

Figure 2. Sketck demonstrating the measured flow parameters.

The peak-to-trough amplitude of core velocity $\hat{U}_{cl}$ downstream of the nozzle exit are presented in a nondimensional form, versus the frequency (f) for nozzles with different area ratios as shown in Figure (4).

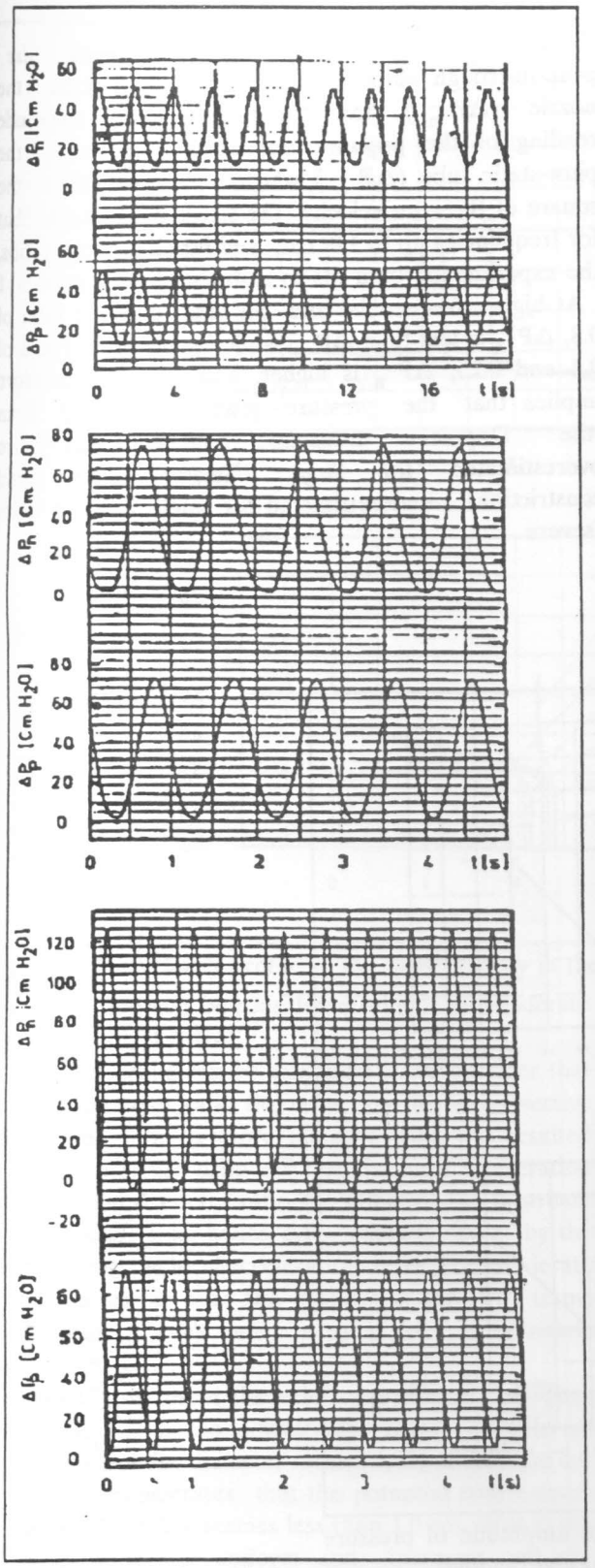

Figure 3. Samples of the recorded signals of the pressure drop across the nozzle P_n and the Pitot tube reading P_p.

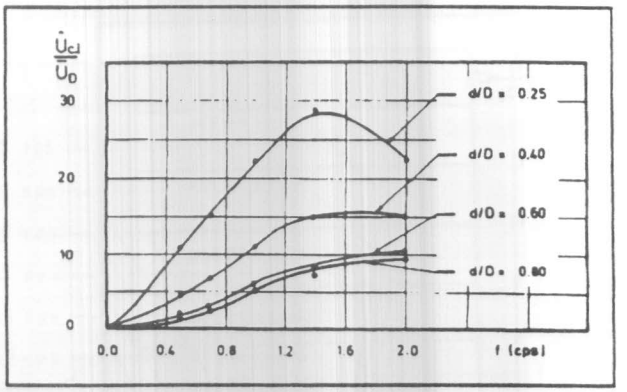

Figure 4. The peakk-to trough amplitude of the center line velocity downstream the nozzle exit.

The figure shows a consistent increase in velocity with increasing the frequency for mild constriction (d/D > 0.6. However, for severe constrictions (d/D $\leq$ 0.4), the periodic core velocity starts to decline at high frequencies

Since, the amplitude of the periodic velocity component is directly proportional to the angular velocity of the pulsator, the drop in U_{cl} beyound a certain frequency at severe constrictions may be attributed to the reflection of pressure and flow waves at the constriction site. These waves occur in pulsatile flow when there is a change in the characteristic admittance of the transmitting tube [23]. The transmitted flow wave downstream of the nozzle in this case will be less than the incident flow wave by the amount of the reflected flow at the constriction. As (d/D) decreases, closed end reflection is approached i.e. the reflected pressure wave approaches the value of the incident pressure wave causing the transmitted flow wave to diminish. The effect of wave reflection was also recognized by Newman [24] and Farran [25] in their in-vivo studies and confirmed by Rooz [26] and Pedly [27].

Figure(5) represents, the variation of peak-to-trough amplitude of oscillating pressure drop across the constriction (ΔP_n) as a function of the nozzle's diameter ratio (d/D) at different frequencies. The figure shows that ΔP_n decreases as the diameter ratio increases. For severe constriction the rate of change of ΔP is drastic and decreases gradually till it becomes very small at mild constriction. The drastic gradient of the curve in the case of severe constriction is due to the contribution of the convective acceleration term to the pressure gradient. This term starts to diminish for larger values of the area ratio, since it is proportional to $(1 - (d/D)^4)$.

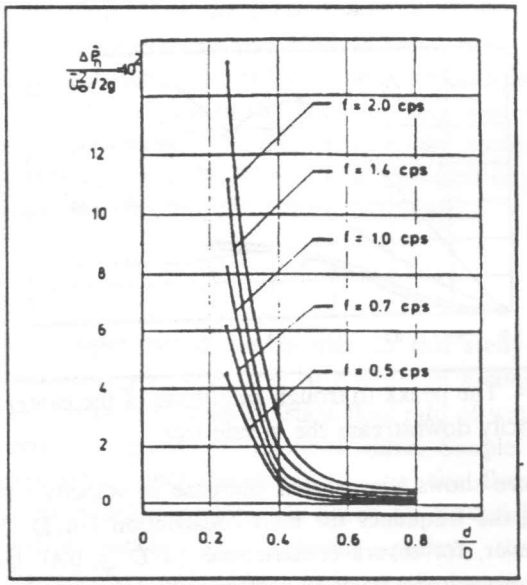

Figure 5. The peak-to-trough amplitude of oscillating pressure drop across the nozzle.

Figure (6) shows a comparison between the peak-to-trough amplitude of pressure drop across the nozzle (ΔP_n) and the peak-to-trough amplitude reading of the pressure transducer connected to the pitot-static tube (ΔP_n) which is proportional to the square of the core velocity. The figure demonstrates that for frequencies up to 1.0 cps, and for all diameter ratios, the experimental data fits to a straight line of slope = 1. At higher frequencies and for the diameter ratio of 0.8, ΔP_n is less than ΔP_p, while for diameter ratios of 0.4 and 0.25, ΔP_n is higher. The results therefore implies that the pressure gradient estimated from the Doppler ultrasound measurements are overestimated for large diameter ratios (mild constriction), underestimated for small diameter ratios (severe

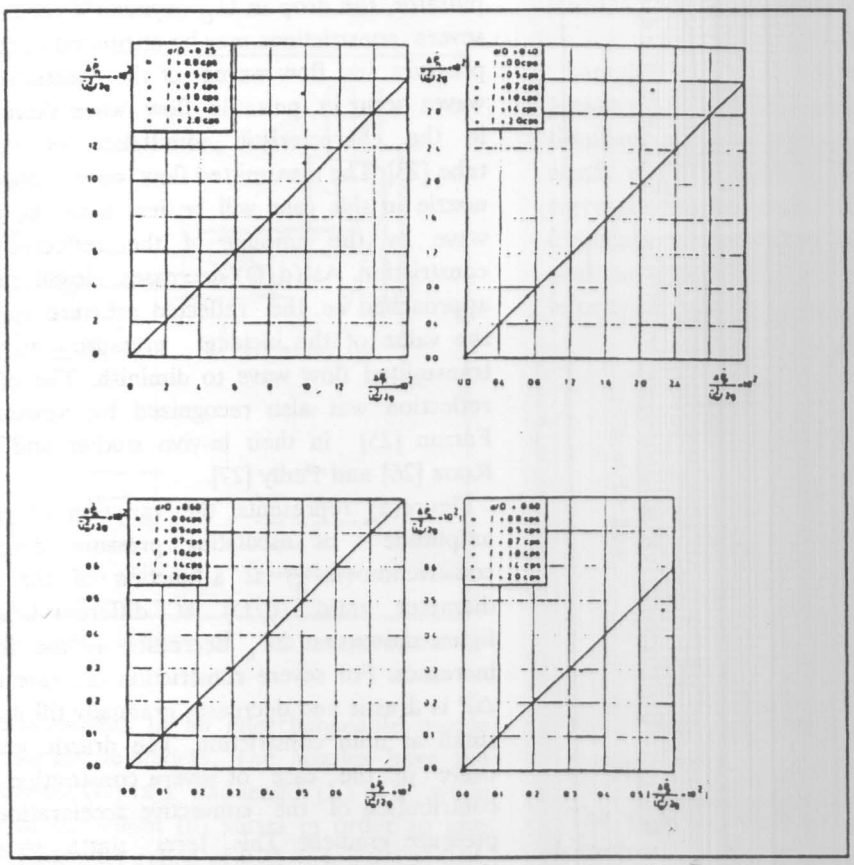

Figure 6. A comparison between the peak-trough amplitude of pressure drop across the nozzel and that of the pitot-static tube reading.

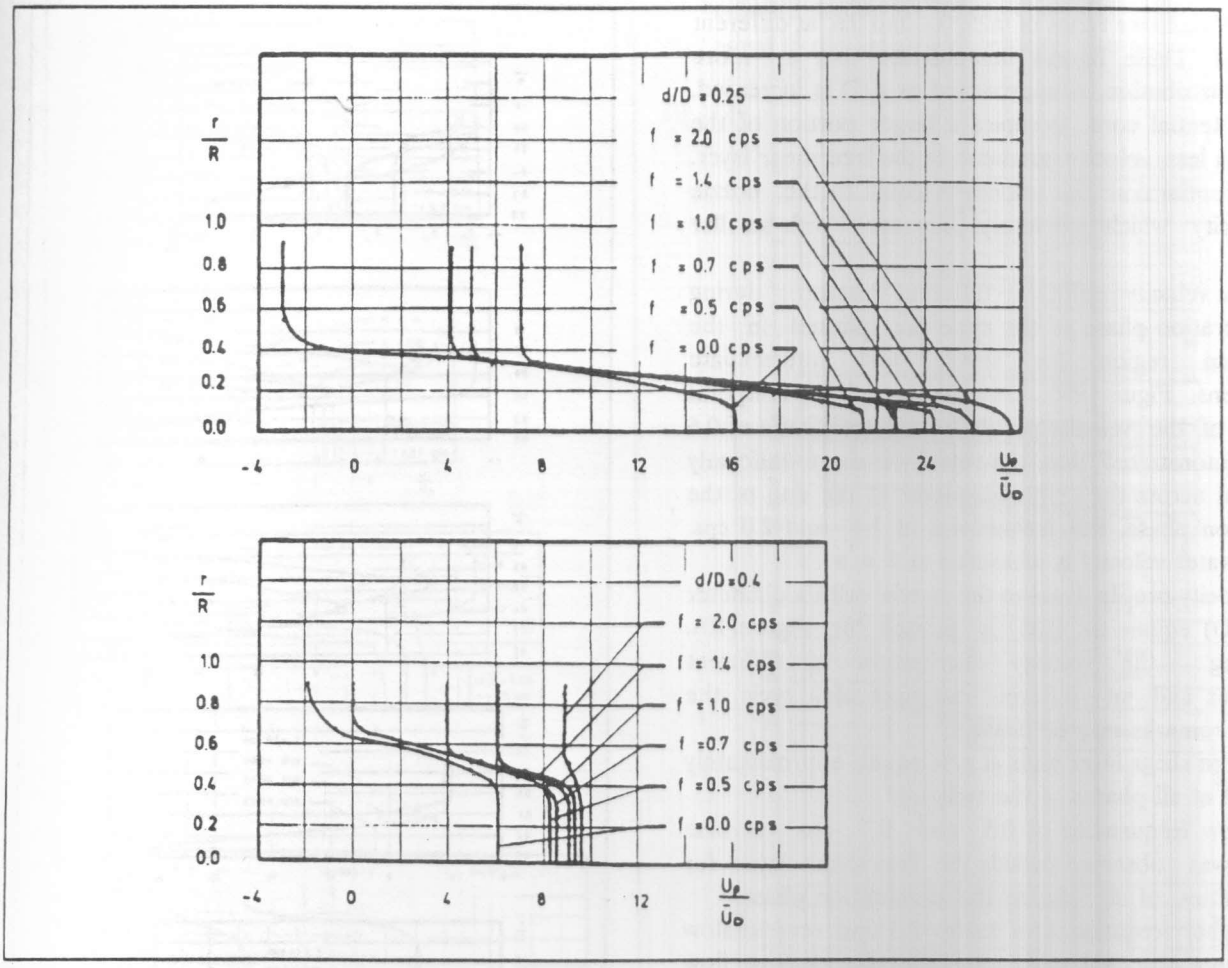

Figure 7. The velocity profile of the peak velocity in the downstream region a) d/D = 0.25 b) d/D = 0.4

constriction) and may be considered reliable for moderate constrictions (d/D ≈ 0.6).

The above results can be explained if we consider that for large diameter ratio the reduction of the convective acceleration term is more effective than the resulted increase of pressure drop ΔP by the local acceleration term. At small diameter ratio the effect of the upstream velocity is neglegible, hence ΔP_n exceeds ΔP_p by the contribution of the local acceleration term. For moderate values of diameter ratio the changes in the two terms counter balance each other causing ΔP_n to be nearly equal to ΔP_p.

Figures (7) represent the velocity profile of the peak velocity (U_p) - in the downstream region at different frequencies and for diameter ratios (d/D) of 0.25 and 0.4. Figure(7-a)demonstrates that the potential core extends to r/R = 0.1 for frequencies less than 1.0 cps. Within this core, the velocity is uniform and increases with the frequency of pulsations. Between r/R equals to 0.1 and 0.4 i.e. in the free shear layer the velocity drops sharply for all frequencies. In recirculation regions uniform velocities are observed and have negative values at low frequencies ,implying that the flow is reversed in this region of the flow field.

In Figure(7-b) where the diameter ratio (d/D) is 0.4 the maximum velocities accur at r/R less than 0.4 and is also uniform along this region of the pipe for all frequencies. The free shear layer extends between r/R equals to 0.4 to 0.6. It was also observed that increasing the frequency results in a lower velocity gradient across this region of the pipe. Beyond r/R = 0.6 uniform velocity occurs and a reverse flow is observed at steady flow conditions (f=0), while stationary flow occurs at frequencies of 0.5 and 0.7 cps. For the higher frequencies the peak velocity in the recirculation region is positive and also increases with the frequency of pulsation .

Figures (8a-8f) represent the velocity profile for

nozzles of diameter ratios of 0.25, 0.4 and 0.6, at different frequencies. These figures demonstrate that a more uniform distribution is approached as d/D is increased, i.e. the potential core occupies a larger portion of the field with a less velocity gradient in the free shear layer. In the potential core the velocity is equal to the nozzle exit velocity which obviously increases with smaller area ratio .

The axial velocity profiles at different instances during the acceleration phase of the cycle are plotted in the downstream region for severe and intermidiate constrictions. Figure (9) represents the temporal variation of the velocity profile for diameter ratio of 0.6 which demonstrates that the velocity is more uniformly distributed across the pipe diameter at the end of the acceleration phase. For frequencies of 1.4 and 2.0 cps. uniform water velocity is measured at $\theta = \pi$.

The velocity profile distal to the nozzle with a diameter ratio (d/D) equal to 0.25 is plotted in Figure(10). Comparing the velocity distribution at different frequencies and at different instances of a cycle, the following remarks may be drawn:

1. The free shear layer ends at r/R equals approximately to 0.4 at all phases of the cycle .
2. For low frequencies of 0.5 and 0.7 cps. reverse flow was observed outside the free shear layer for all values of θ, during the acceleration phase
3. At higher frequencies of 1.0 to 2.0 cps. reverse flow was only observed at $\theta = 0$, otherwise positive flow was measured in the recirculation region .
4. At low frequencies the width of the potential core is constant throughout the cycle. However, for higher frequencies as the flow accelerates the potential core ceases to exist at same downstream section..
5. As the frequency increases the whole velocity profile is shifted during the acceleration phase. At lower frequencies the potential core velocities increase while the minimum velocity in the recirculation region remains constant, which results in a higher shearing of the fluid in the free shear layer [i.e. higher velocity gradient as the phase angle (θ) increases] .

Plotting the instantaneous values of the pressure drop across the nozzle against the instantaneous values of the flow rate, during one complete period of oscilation, demonstrates the phase shift between the pressure gradient and the velocity signal as shown in Figures (11,12). The width of the loop which is a function of the phase shift increases with increasing the area ratio or the frequency of pulsations.

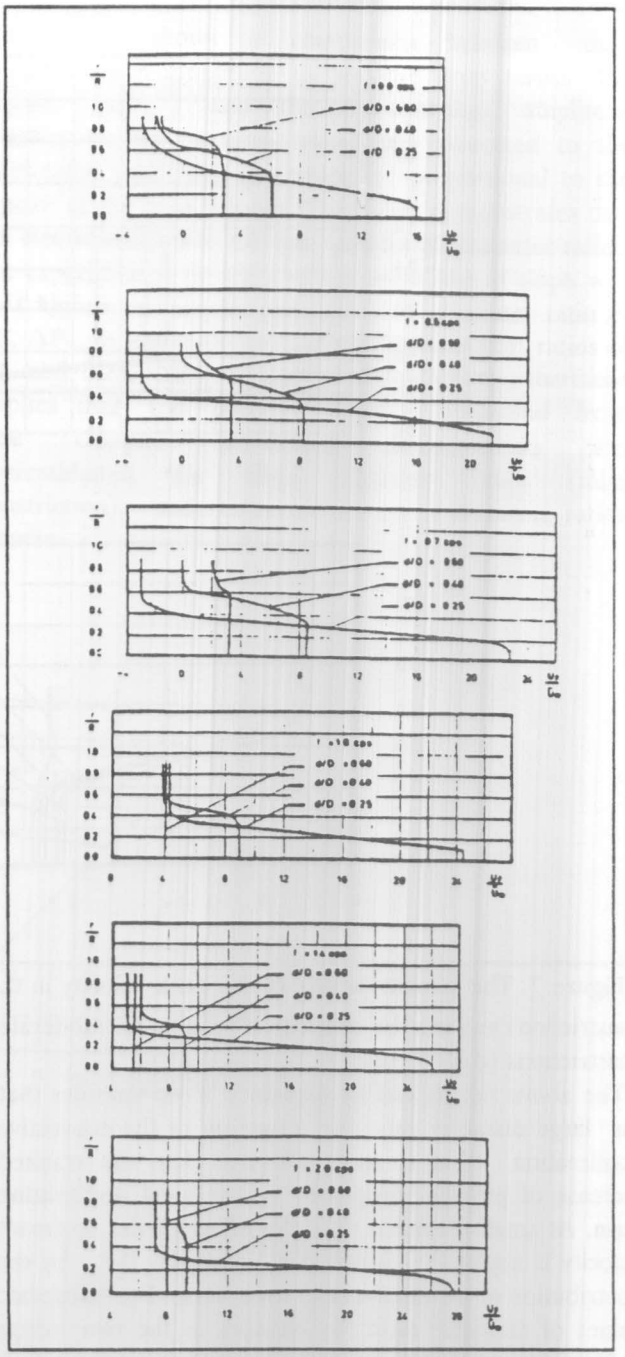

Figure 8. The velocity profiles for different nozzles at different frequencies.

From the previous discussion it may be stated that the general structure of the pulsatile flow field downstrean of

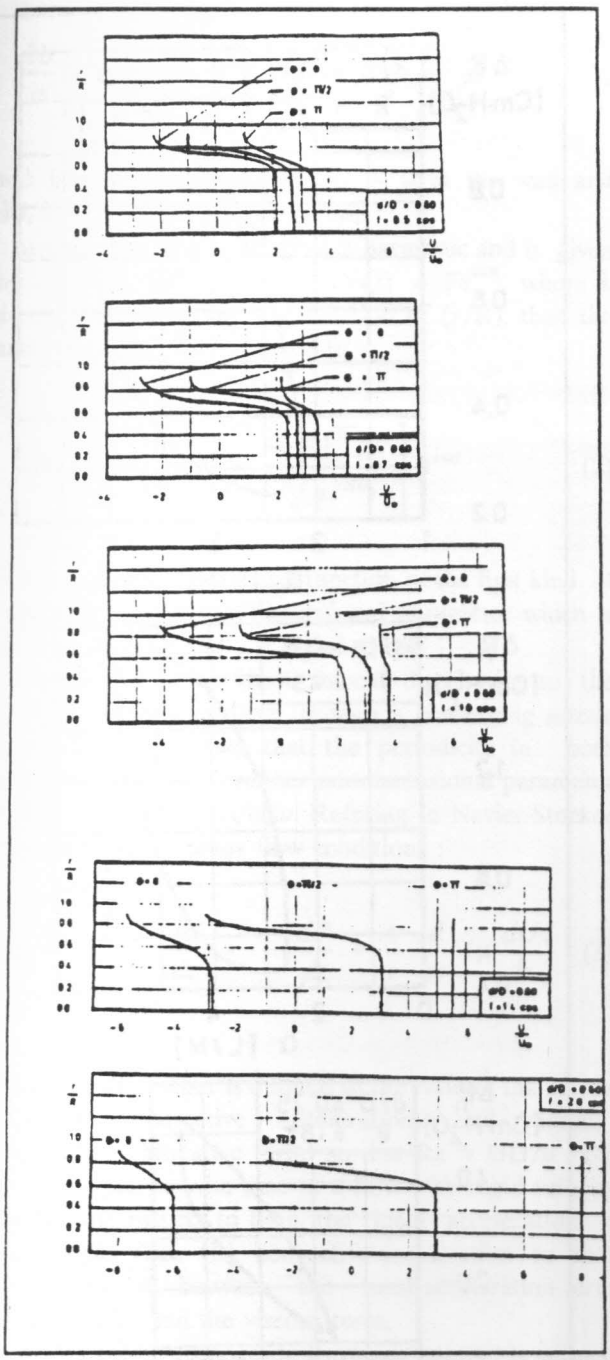

Figure 9. Temporal variation of velocity profile for d/D = 0.6 at different frequencies.

a nozzle is similar to that of a steady confined jet issuing through a convergent nozzle .

Downstream of the nozzle exit, an annular moving layer forms between the potetial core and the surrounding fluid. This layer spreads along the flow until it fills the entire tube. Within the potential core the velocity profile is nearly uniform and the velocity is equal to the nozzle exit velocity. The potential core length

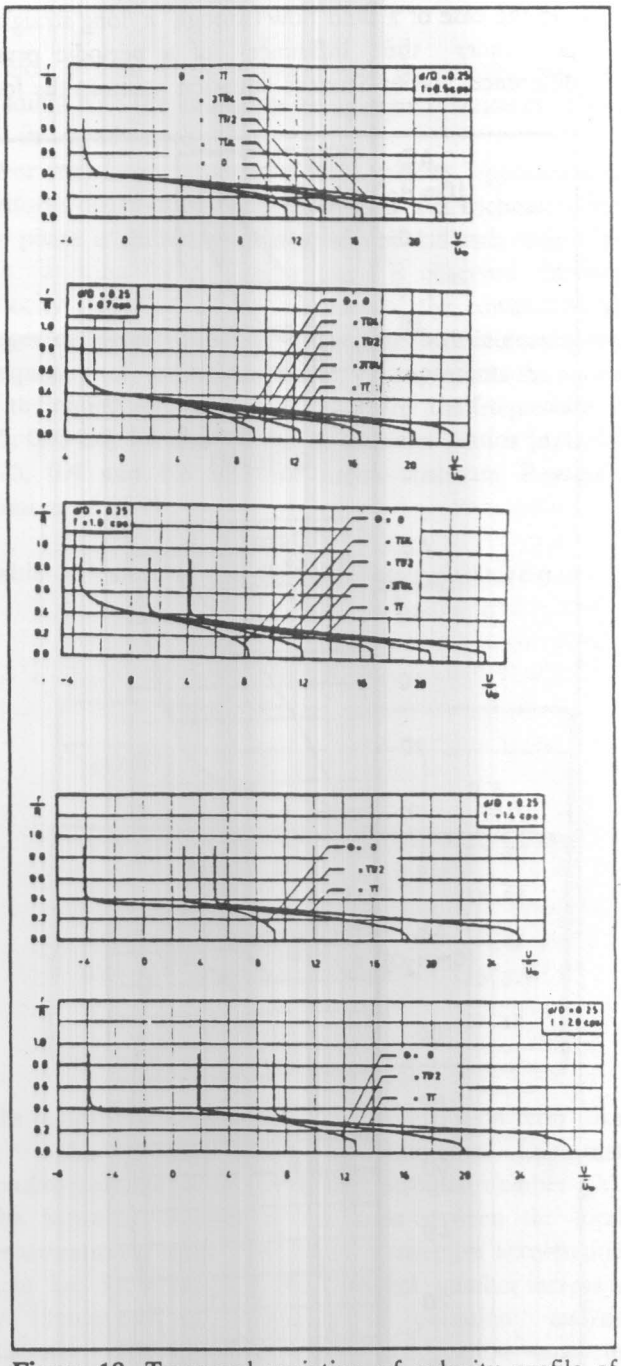

Figure 10. Temporal variation of velocity profile of d/D = 0.25 at different frequencies.

is about 5 to 6 the nozzle exit diameter .

In order to understand the effect of oscillation on the

flow across the entire pipe cross-section, it might be worthwile to review some of the gross features of the oscillating flow through pipes .

In the case of a fluid flow through a long straight rigid pipe under the influence of a periodic pressure difference, Navier-Stockes equation assumes the form,

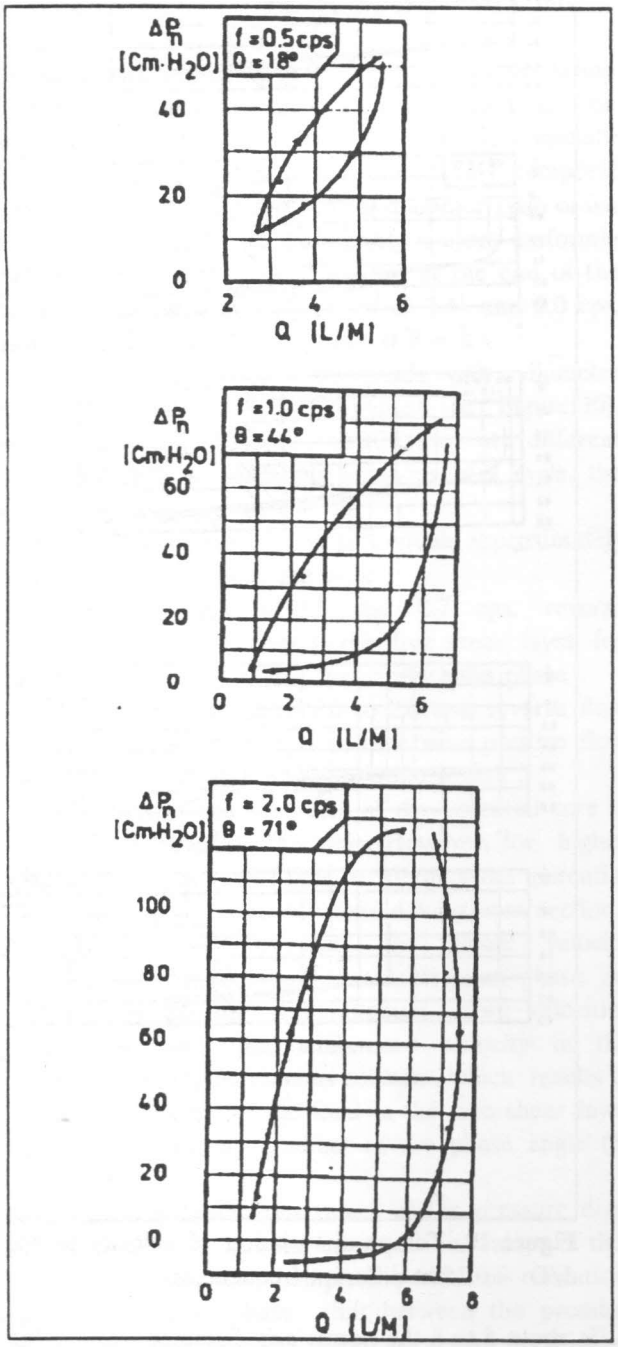

Figure 11. Instantaneous pressure drop versus instantaneous discharge for d/D = 0.25.

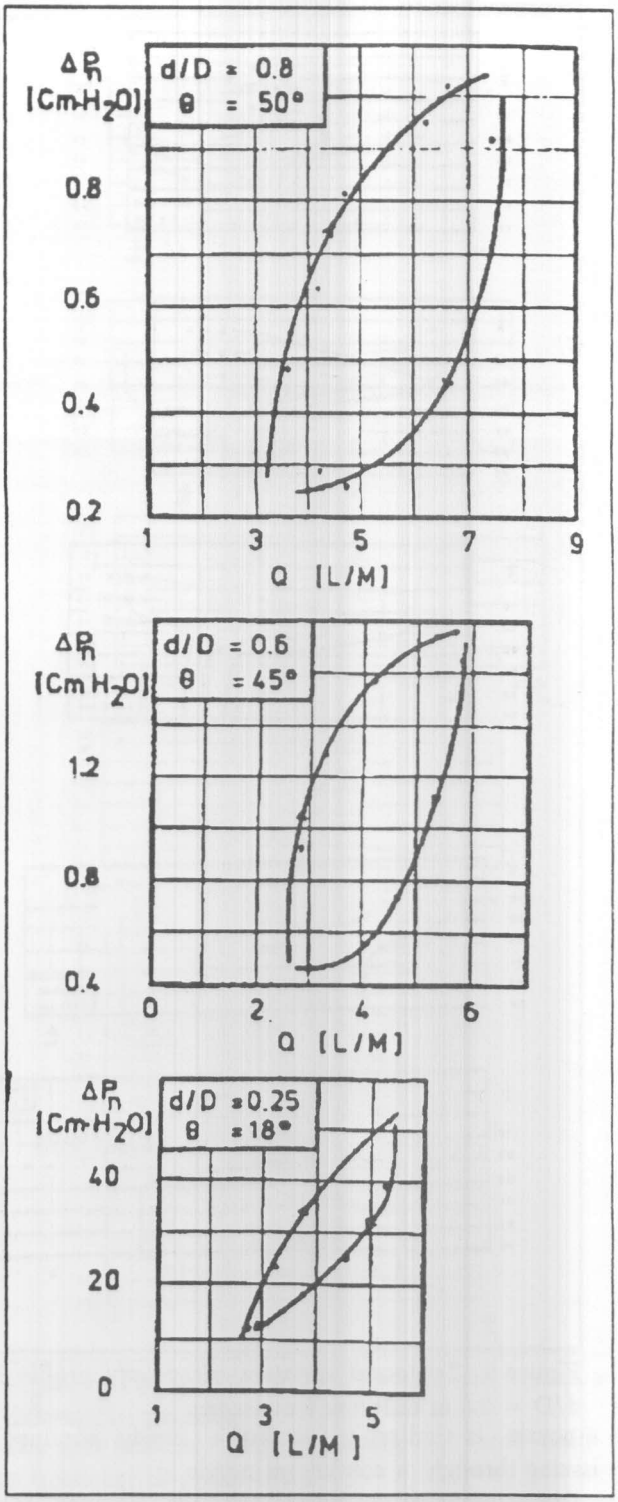

Figure 12. Instantaneous pressure drop versus instantaneous discharge for f = 0.5 cps.

$$\frac{\partial U}{\partial t} = -\frac{1}{\rho}\frac{\partial P}{dz} + \nu\left(\frac{\partial^2 U}{\partial r^2} + \frac{1}{r}\frac{\partial U}{\partial r}\right) \quad (1)$$

with boundary conditions of U = 0 at the wall and $\partial U/\partial r = 0$ at the pipe centreline.

Assuming the pressue gradient is harmonic and is given by $\partial P/\partial z = Ke^{i\omega t}$ and that $U(r,t) = Fe^{i\omega t}$, where k denotes a constant and F a function of (r/R), then the axial velocity (U) will be equal to :

$$U(r,t) = \frac{iK}{\rho\omega}\left[1 - \frac{J_o(\alpha i^{3/2} y)}{J_o(\alpha i^{3/2})}\right] e^{i\omega t} \quad (2)$$

Where J_0 denotes the Bessel function of the first kind of order zero , α is a non-dimensional parameter which is equal to $R\sqrt{\omega/\upsilon}$ and y is equal to r/R .

The relevance of the above velocity distribution to the problem of oscillating flow through a converging nozzle stems from the fact that the periodicity in both problems introduces another nondimensional parameter a which is equal to $R\sqrt{\omega/\upsilon}$. Refering to Navier-Stockes equation under unsteady flow conditions :

$$\rho\frac{du}{dt} + \rho U\frac{dU}{dz} = -\frac{dP}{dz} + \frac{1}{r}\frac{d}{dr}\left(\mu\frac{dU}{dr}\right) \quad (3)$$

The Reynolds number is defined as the ratio of the inertia force term (convective acceleration) and viscous force term (dissipative term) so that $Re \simeq UD/\upsilon$. On the other hand in the case of a flow with rapid velocity variation wih respect to time, the local acceleration is much larger than the convective acceleration so that the balance is between the local acceleration term $\partial U/\partial t$ or $[\omega U]$ and the viscous term.

Therefore, the corresponding Reynolds number is defined as $\omega D^2/\upsilon$ which is eqal to α^2 . Hence the parameter α may be considered as a kind of unsteady Reynolds number for unsteady flow as it indicates the relative importance of inertial and viscous forces in determining the motion within the time scale of one period of an oscillation, and is denoted as a frequency parameter.

The two limiting cases of very large and very small α prove to be very simple. For small α the velocity is

$$U(r,t) = \frac{K}{4\mu}(R^2 - r^2)\cos\omega t \quad (4)$$

Which is seen to be in-phase with the exciting pressure gradient with the amplitude being same function of radius as in steady state .

For very large values of α the velocity approaches a uniform distribution (bulk flow) as if it is frictionless and its phase is shifted by quarter of a period with respect to the exciting force. Similar trend is observed in the velocity distribution downstream of the constriction at larger diameter ratios of 0.4 and 0.6 with increasing the frequency of pulsation. Table (1) represents the values of the dimensionless parameter α for the frequencies of 0.5, 0.7, 1.0, 1.4 and 2.0 cps at diameter ratios (d/D) of 0.25, 0.4 and 0.6 and for mean upstream Reynold's number of 3340 .

Table 1. Values of the dimensionless parameter α.

(α)			
(d/D) / (f)	0.25	0.4	0.6
0.5	5.76	9.49	13.90
0.7	6.82	11.23	16.44
1.0	8.16	13.41	19.67
1.4	9.64	15.87	23.27
2.0	11.51	18.97	27.82

In periodic flow with convective acceleration term like in the present study an additional important nondimensional parameter is the Strouhal number (St). The Strouhal number is the ratio between the local acceleration term to the convective acceleration term i.e. $St. \simeq [\omega D/U]$. As Strouhal number increases by increasing the frequency of pulsation and/or diameter ratio, the convective acceleration term in equation (3) can be neglected and the equation reduces to that for a flow in a pipe under oscillating pressure gradient. On the other hand, for very small oscillation and/or severe constriction the equation is reduced to that of a steady state flow conditions through a nozzle.

Carrying out the experiment for different diameter ratios and different frequencies allowed these trends to be observed .

CONCLUSIONS

With reference to the previous discussion of the experimental results, the following conclusions may be drawn :

1. Any reduction in the diameter ratio of the constricted area has a significant effect on the value of pressure drop measured across the constriction for diameter ratio below 0.4, while for diameter ratio more than 0.6 the area change has no significant effect .
2. At high frequencies, the Doppler technique in which the local acceleration term is neglected, leads to overestimated values of pressure drop across mild constriction and to underestimated values for severe constrictions .
3. For large Strouhal number, the flow is similar to that in a pipe under oscillating pressure gradient. On the other hand for small Strouhal number, the flow is similar to that of steady flow through a confined nozzle .
4. The core velocity increases by increasing the frequency of pulsation and/or decreasing the area of the constriction .
5. For large frequency parameter, the velocity profile has nearly uniform shape (bulk flow) and its lagging phase angle from the pressure drop approaches $\pi/2$.
6. At low frequencies, the potential core velocity increases while the minimum velocity remains constant resulting in higher shearing of the fluid in the free shear layer. As the frequency increases the whole velocity profile is shifted during the acceleration phase keeping nearly constant shearing of the fluid in the free shear layer.

REFERENCES

[1] Dow. J.W., Levin, H.D., Elkin, M., Haynes, F.W., Hellems, H.K., Whittenberger, J.W., Ferris, B.G., Goodale, W.T., Harvey, W.P., Eppinger, E.C., and Dexter, L., "Studies of Congential Heart Disease, (IV) Uncomplicated Pulmonic Stenosis", *Circulation*, vol. 1, pp 269:287, 1950.

[2] Gorlin, R., and Gorlin, S.G, "Hydraulic Formula for Calculation of the Area of the Stenotic Mitral Valve, Other Cardiac Valves, and Central Circulatory Shunts", *I. Am. Heart J.*, vol. 41, No. 1; pp 1:29; 1951.

[3] Berger H.C., Bremmelen A.G. and Dannenburg F.J., "Theory and experiments on Schematical Models of stenosis", *Cir. Res.*, vol. 4 pp. 425:429, 1956.

[4] Forrester J.H. and Young D.F., "Flow through a converging-Diverging tube and its implications in occlusive vascular diseases", *J. Biomechanics* vol. 3, pp 297:316, 1970.

[5] Seeley B.D. and Young D.F., "Effect of Geometry or pressure losses across Models of arterial stenoses", *J. Biomechanics*, vol. 9, pp 349:448, 1976.

[6] Ojha, Matadial; Cobbold, Richard S.C.: Johnston, K. Wayne and Hummel, Richard L. "Pulsatile flow through constricted tubes: an experimental investigation using photochromic tracer methods", *J. Fluid Mech.* v 203, pp 173-197, 1989.

[7] Lee, J.S. and Fung, Y.C.,"Flow in locally constricted tubes at low Reynolds numbers", *J. appl. Mech.*, 37, 9-16 1970.

[8] Hung, T.K., "Vortices in pulsatile flow", *Proc. Ist. Int. Conf. Rheology 2*, 115-127, 1971.

[9] Cheng L.C., Robertson J.M. and Clark M.E., "Numerical Calculations of plane oscillatory non uniform Flow-II. Parametric study of pressure gradient and frequency with square wall obstacles", *J. Biomechanics* 6, 521-538, 1973.

[10] DALY B.J., "A numerical study of pulsatile flow through strenosed canine fenoral arteries", *J. Biomechanics* 4, 465-475, 1976.

[11] Deshpande M.D., Giddens D.P. and Mabon R.F., "Steady laminar flow through Modelled vascular stenoses", *J. Biomechanics* n:9, 165-174, 1976.

[12] Less, R.S. and Dewey, C.F., "Phonoangiography a new non-invasive diagnostic method for studying arterial disease", *Proc. Nat. Acad. Sci.* 67, 935-942, 1970.

[13] Young, D.F. and Tsai, F.Y., "Flow characteristics in models of arterial stenoses-I. Steady flow", *J. Biomechanics* n:6, 395-410, 1973.

[14] Kim, B.M. and Corcoran, W.H., "Experimental measurements of turbulence spectra distal to stenosis", *J. Biomechanics*, 7, 335-342, 1974.

[15] Clark C., "Turbulent velocity measurements in a model of aortic stenosis", *J. Biomechanics* 4, 677-687, 1976.

[16] Abdallah S.A., Hwang N.H.C., "Arterial stenosis murmurs: An analysis of flow and pressure fields", *J. Acoust. Soc. Am.* 83 (1) pp. 318: 334, 1988.

[17] Hatle, L., Angelsen, B.A., and Tramsdal, A., "Noninvasive Assessment of Aortic Stenosis by Doppler Ultrasound", *Br. Heart J.*, vol. 43, pp 284:292, 1980.

[18] Stamm, R.B., and Martin, R.P., "Quantification of pressure Gradients Across Stenotic Valves by Doppler Ultrasound", *J. Am. Coll. Cardiol.*, vol. 2, pp 707:718. 1983.

[19] Berger, M., Berdoff, R.L., Gallerstein, P.E.,and Goldberg, F., "Evaluation of Aortic Stenosis by Continuous Wave Doppler Ultrasound", *J. Am. Coll. Cardiol*, vol. 3, pp 150:156, 1984.

[20] Currie, P.J. Seward, J.B., Reeder, G.S., Vlietstra, R.E., Bresnahan, D.R., Bresnahan, J.B., Smith, H.C., Hagler, D.J., and Tajik, A.J., "Continuous wave Doppler Echocardiographic Assessment of Severity of Calcific Aortic Stenosis A Simultaneous Doppler-Catheter Correlative Study in 100 Adult Patients", *Circulation*. vol. 71. No. 6, p 1162:1169, 1985.

[21] Panidis, I.P., Mintz, G.S., and Ross, J., "Value and Limitations of Doppler Ulttrasound in the Evaluation of Aortic Stenosis: A Statistical Analysis of 70 Consecative Patients", *Am. Heart J.*, vol. 112, No. 1, pp 150:158, 1986.

[22] Requarth, J.A., Goldberg, S.J., Vasko, S.D., and Allen, "Transvalve Pressure Gradient and Orifice Area in Stenosis", *Am. J. Cardiol.*, vol. 53, pp 1369:1373, 1984.

[23] McDonald, D.A.: "*Blood Flow in Arteries*", The Camelot Press Ltd, Southampton, 1974.

[24] Newman, D.L., Batten, J.R. and Bowden, N.L.R., "Partial standing wave formation above an abdominal aortic stenosis", *Cardiovascular Res.*, vol. 11, pp 160-166, 1977.

[25] Farrar, D.J., Green, H.D. and Peterson, D.W., "Noninvasively and invasively measured pulsatile haemodynamics with graded arterial stenosis", *Cardiovascular Res.*, vol. 13, pp 45-57, 1979.

[26] Rooz, E., Young, D.F. and Rogge,T.R., " A Finite element simulation of pulsatile flow in flexible obstructed tubes", *J. Biomech. Eng.*, vol. 104, pp 119-124, 1982.

[27] Pedley, T.J., "Non-linear pulse Wave Reflection at an Arterial Stenosis" *J. Biomech. Eng. Trans. (ASME)*, vol. 105, No. 4, pp 335-359, 1984.